

Quantitative Imaging Markers on HRCT Predict Rapid Progression and Adverse Events of Patients with Idiopathic Inflammatory Myopathies-Related Interstitial Lung Disease

Hongyi Wang^{1,2,*}, Yuhui Qiang^{2-4,*}, Jianping Wang^{3,5}, Yifei Ni^{1,5}, Anqi Liu^{1,5}, Jie Du^{1,5}, Yanhong Ren², Shiyao Wang², Jing Geng², Bingbing Xie², Min Liu⁵, Huaping Dai²

¹China-Japan Friendship Hospital (Institute of Clinical Medical Sciences), Chinese Academy of Medical Sciences & Peking Union Medical College, Beijing, People's Republic of China; ²Department of Pulmonary and Critical Care Medicine, National Center for Respiratory Medicine; State Key Laboratory of Respiratory Health and Multimorbidity; National Clinical Research Center for Respiratory Diseases; Institute of Respiratory Medicine; Chinese Academy of Medical Sciences; Center of Respiratory Medicine; China-Japan Friendship Hospital, Beijing, People's Republic of China; ³Capital Medical University, Beijing, People's Republic of China; ⁴Immune Dysfunction and Pulmonary Fibrosis Joint Laboratory for Clinical Medicine, Capital Medical University, Beijing, People's Republic of China; ⁵Department of Radiology, China-Japan Friendship Hospital, Beijing, People's Republic of China

*These authors contributed equally to this work

Correspondence: Min Liu, Department of Radiology, China-Japan Friendship Hospital, Yinghua Dong Street, Hepingli, Chao Yang District, Beijing, 100029, People's Republic of China, Email mikie0763@126.com; Huaping Dai, Department of Pulmonary and Critical Care Medicine, China-Japan Friendship Hospital, Yinghua Dong Street, Hepingli, Chao Yang District, Beijing, 100029, People's Republic of China, Email daihuaping@ccmu.edu.cn

Objective: To assess imaging quantitative markers on baseline High-resolution computed tomography (HRCT) for predicting rapid progression (RP) and adverse events in anti-synthetase syndrome associated interstitial lung disease (ASS-ILD) and anti-MDA5-positive dermatomyositis-associated interstitial lung disease (MDA5-ILD).

Methods: This retrospective study analyzed 511 patients (ASS-ILD: n=356, median age=56 years; MDA5-ILD: n=155, median age=50 years) between Jan 2016 and Dec 2021. RP was defined as pulmonary function, image, or symptom aggravation within 3 months of initial presentation. Adverse events (death/intensive care) were recorded. Deep learning quantified ground-glass opacity (GGO) and consolidation volumes/percentages on baseline HRCT. Multivariable logistic and Cox regression adjusted for confounders (age, gender, smoking status, body mass index, fibrosis, and treatment). No multiple comparisons were conducted since this is an exploratory study.

Results: RP occurred in 34.8% (124/356) of ASS-ILD and 44.5% (69/155) of MDA5-ILD patients. Elevated GGO/consolidation volumes and percentages independently predicted RP in patients with ASS-ILD (adjusted odd ratio=1.63, 95% confidence interval: 1.25–2.12, $P<0.001$), but not in patients with MDA5-ILD. During median follow-up (ASS-ILD: 4.45 years; MDA5-ILD: 4.05 years), RP patients showed higher mortality versus patients without RP (hazard ratio=4.12, $P<0.001$). Increased baseline GGO/consolidation metrics predicted adverse events in patients with ASS-ILD or MDA5-ILD ($P<0.01$).

Conclusion: GGO and consolidation quantification on baseline HRCT can provide clinically actionable predictors to identify patients with ASS-ILD at high-risk for RP, and to stratify adverse event risks across ASS/MDA5-ILD regardless of RP status, enabling early intervention.

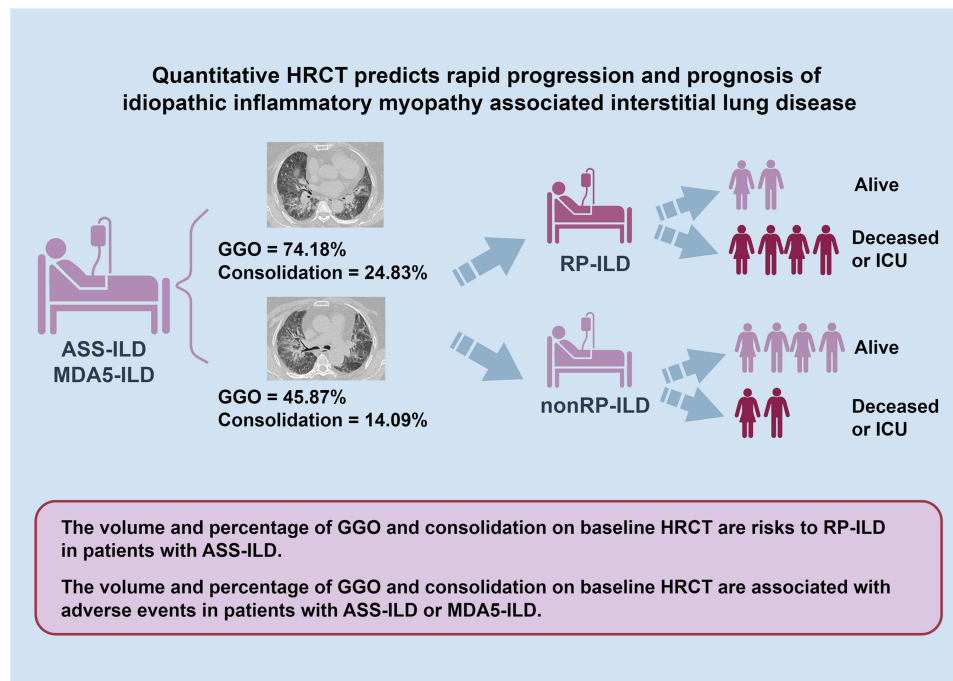
Keywords: idiopathic inflammatory myopathy, anti-synthetase syndrome, anti-MDA5-positive dermatomyositis, high-resolution computed tomography, ground-glass opacity, consolidation, rapidly progressive interstitial lung disease

Introduction

Rapidly progressive interstitial lung disease (RP-ILD) is characterized by worsening symptoms, image progression, and impaired pulmonary function in patients with idiopathic inflammatory myopathy (IIM)-related interstitial lung disease (ILD), leading to increased mortality and a low life quality.¹ Anti-synthetase syndrome (ASS) and anti-MDA5-positive dermatomyositis (MDA5) are important clinical subtypes of IIM that have been reported to be closely related to ILD.^{2–6}



Graphical Abstract



Current concepts emphasize that ASS, characterized primarily by antibodies against aminoacyl-tRNA synthetases, frequently manifests ILD as a cardinal feature, often preceding or overshadowing myositis.⁷ Conversely, MDA5 defines a unique subset often presenting with clinically amyopathic dermatomyositis and carries a significant risk for RP-ILD. The prevalence of ILD in patients with ASS exceeds 80%,^{8,9} and the incidence of ILD in patients with MDA5 can be as high as 90%. Most importantly, approximately 80% of MDA5-related ILD (MDA5-ILD) patients and 7.8%–8.9% of patients with ASS-related ILD (ASS-ILD) were reported to exhibit RP-ILD.^{10,11} The mortality rate among patients with IIM-related ILD (IIM-ILD) is reported to be 70%–90% in those with RP-ILD.^{12–14} If recognized early, RP-ILD can be treated with appropriate immunosuppressive therapy to optimize patients' prognosis.¹⁵ Thus, prediction of RP-ILD is crucial for both ASS-ILD and MDA5-ILD management.

High-resolution computed tomography (HRCT) has been widely used in the evaluation of IIM-ILD. Ground glass opacities (GGO) and consolidation are the most common imaging findings in ASS-ILD and MDA5-ILD.^{16–18} ASS-ILD typically presents with a subacute onset and exhibits a mixed pattern of nonspecific interstitial pneumonia, and/or organizing pneumonia on HRCT.⁷ MDA5-ILD is notoriously aggressive, characterized radiologically by rapid progression of GGO and consolidation. However, the correlation between quantitative GGO or consolidation with RP-ILD and the prognosis remains unclear. While HRCT is routinely integrated with pulmonary function tests, symptom acuity, and serum biomarkers (such as ferritin, lactate dehydrogenase, and Krebs von den Lungen 6) in multi-modal assessments aimed at stratifying the risk of RP-ILD.¹⁹ Inadequate understandings of HRCT features and RP-ILD limits the predictive power of current multi-modal approaches. In recent years, quantitative CT (QCT) has emerged as an assessment tool for ILD progression and is more accurate than visual assessment.^{20,21} QCT assessments can also facilitate the reliable and accurate diagnosis, monitoring, and prognosis of lung diseases.^{22,23} We hypothesized that the quantitative features of GGO and consolidation on QCT are associated with RP-ILD or a poor prognosis. In this study, we aimed to comprehensively analyze the clinical and quantitative features of HRCT to identify the risk factors associated with RP-ILD and prognosis in patients with ASS-ILD and MDA5-ILD.

Methods and Materials

Study Design and Population

The study protocol was approved by the Ethics Committee of China-Japan Friendship Hospital (No. 2017–25) and was retrospectively analyzed based on the registered perspective cohort (NCT04370158). Our study complies with the Declaration of Helsinki. Written informed consent was obtained from all the patients. Patients diagnosed with ASS-ILD or MDA5-ILD at our hospital between Jan 2016 and Dec 2021 were included in the study. The identification and classification of IIM was based on the criteria established by Bohan and Peter.²⁴ The diagnostic criteria employed for ASS and MDA5 were the classification criteria established by the 2018 European Neuromuscular Centre dermatomyositis criteria.²⁵ To diagnose ILD, we followed the guidelines of the American Thoracic Society/European Respiratory Society guidelines.²⁶ The diagnosis of ASS-ILD or MDA5-ILD was made through multidisciplinary discussion (MDD). The exclusion criteria were as follows: (1) patients without baseline HRCT or HRCT with poor image quality during hospitalization, and (2) concurrent malignancy or heart failure based on electronic records.

The diagnostic criteria for identifying RP-ILD were based on the international consensus, as modified by the declaration of the American Thoracic Society on idiopathic pulmonary fibrosis.²⁷ RP-ILD is confirmed when newly onset at least one of the following criteria is met: (1) aggravation of symptoms, such as exertional dyspnea, (2) augmentation of pulmonary opacification observed on HRCT imaging, and (3) alterations in physiological parameters demonstrated by a decline of 10% in vital capacity (VC) or a decrease of 1.33 kPa in arterial oxygen tension (PaO₂) within individuals affected by IIM-ILD^{28–34} within 3 months since the onset of respiratory symptoms.^{28–34} Adverse events including death and intensive care unit (ICU) admission were derived from electronic medical records or telephone follow-ups. **Figure 1** is the flowchart detailing how participants were selected and grouped. **Figure 1** depicts the prospective screening flowchart of 612 IIM-ILD treated at our Hospital between January 1, 2016 and December 31,

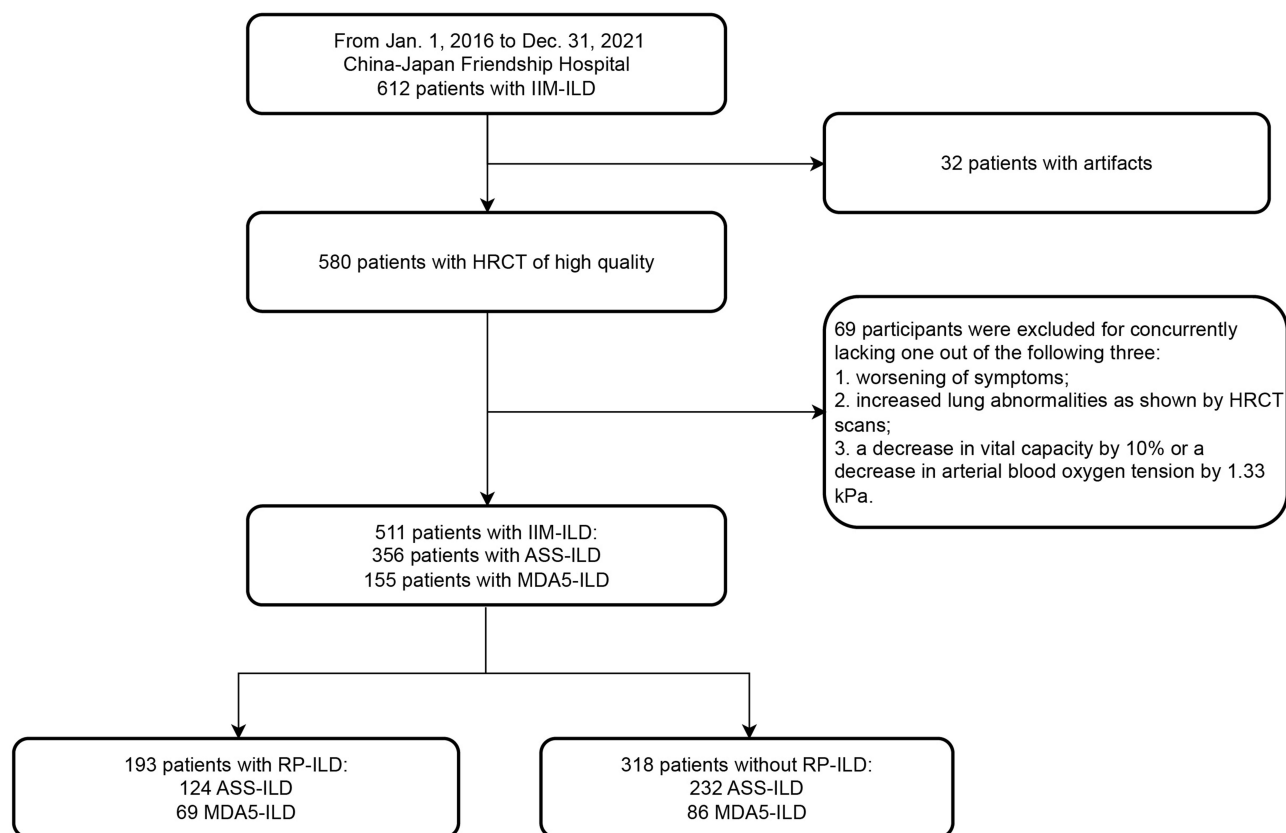


Figure 1 Patient screening flowchart. Prospective enrollment of idiopathic inflammatory myopathy-associated interstitial lung disease (IIM-ILD) patients at China-Japan Friendship Hospital (2016–2021). Boxes indicate critical decision points.

Abbreviations: RP-ILD, rapid progressive interstitial lung disease; ASS-ILD, anti-synthetase syndrome-interstitial lung disease; MDA5-ILD, melanoma differentiation-associated protein 5-positive interstitial lung disease; HRCT, high-resolution computed tomography; IIM-ILD, idiopathic inflammatory myopathy-associated interstitial lung disease.

2021. After excluding 32 subjects with significant imaging artifacts, 580 patients with high-quality baseline HRCT scans were retained. An additional 69 individuals were excluded due to incomplete documentation of at least one of three key progression criteria: (1) respiratory symptom deterioration, (2) radiologically confirmed increase in lung abnormalities, or (3) $\geq 10\%$ decline in VC or ≥ 1.33 kPa reduction in PaO₂. The final cohort comprised 511 patients with IIM-ILD, stratified into 193 RP-ILD cases (124 ASS-ILD; 69 MDA5-ILD) and 318 non-RP-ILD controls (232 ASS-ILD; 86 MDA5-ILD).

Clinical Characters

Demographic factors and pulmonary function assessments were reviewed and extracted from the electronic medical records. Pulmonary function parameters included VC, forced vital capacity (FVC), total lung capacity (TLC), diffusing capacity for carbon monoxide (DL_{CO}), and their percent predicted (VC%, FVC%, TLC%, and DLco%). PaO₂ and arterial carbon dioxide pressure (PaCO₂) were derived from examination of blood gas samples with a specific fraction of inhaled oxygen (FiO₂). Oxygenation index (OI) was defined as PaO₂/FiO₂. The levels of myositis-specific autoantibodies, including anti-nuclear antibody (ANA), anti-RO-52 antibody (RO-52), anti-JO-1 antibody (JO-1), anti-Sjögren's syndrome-related antigen A antibody (SSA), anti-EJ antibody (EJ), anti-Mi-2 antibody (Mi-2), anti-PM-SCL antibody (PM-SCL), and anti-PL-12 antibody (PL-12) were measured by immunoblotting (Euroimmun, Lübeck, Germany). We defined grayscale values < 11 units/L as negative and those ≥ 11 units/L as positive. The exclusion of rare antibodies (PL-7, Zo, etc.) was based on cohort prevalence $< 5\%$ in prior regional studies.

HRCT Scan

All included patients underwent baseline HRCT in the supine position on multilayer spiral CT device (Lightspeed VCT/64, GE Healthcare; Toshiba Aquilion ONE TSX-301C/320; Philips iCT/256; Siemens FLASH Dual Source CT) at the end of inspiration from the lung apex to the lung base. HRCT scanning protocol was spiral mode with the following acquisition and reconstruction parameters included: tube voltage of 100–120 kV, tube current of 100–300 mAs, section thickness of 0.625–1 mm, table speed of 39.37 mm/s, gantry rotation time of 0.8 s, and reconstruction increment of 1–1.25 mm.

CT Analysis

HRCT images in digital-imaging-and-communications-in-medicine format were transferred to an artificial intelligence workstation (FACT AI+—digitalLung V1.0, Shenzhou Dexin Medical Imaging Technology Co., Ltd., Weinan Shanxi, China, <http://www.dexhin.com>),^{35,36} and the lungs were automatically segmented and then corrected by two chest radiologists with 9 and 15 years of experience. The quantitative analysis encompassed a meticulous assessment of GGO and consolidation using pre-trained deep learning. Initially, it segments the GGO and consolidation regions from full-lung images and quantifies their volumes. Subsequently, the percentage of this volume that represents the total lung volume is determined. Within these segmented areas, the corresponding attenuation coefficients are extracted for each voxel, and both the number of voxels with attenuation coefficients exceeding and above the mean value or -300 HU (referred to as the non-solid ratio) were calculated. Finally, the mass of each lesion was computed by multiplying the average voxel value, indicative of the material density within these regions, by their respective volumes. The presence of honeycomb, reticular, or traction bronchiectasis was visually assessed by expert radiologists to classify the fibrosis status ([Supplementary Figure 1](#)).

Statistically Analysis

All statistical analyses and data visualization were performed using R software (version 4.2.2) operating on the Windows 10 platform. The threshold for statistical significance was set at $P < 0.05$ (one-tailed). Multiple Imputation by Chained Equations was used to generate a complete dataset for analysis. We used mean values and standard deviations for continuous variables that were normally distributed. We used medians and interquartile ranges for non-normally distributed data. Categorical variables are presented as numbers and percentages. Data comparisons were performed using t-tests or Mann–Whitney *U*-tests for continuous variables, and chi-square or Fisher's exact tests for categorical variables. Consequently, a multivariable logistic regression model adjusted for the effects of age, sex, body mass index, smoking status, fibrosis status, and treatment history was used to discern QCT features associated with RP-ILD. Associations between pulmonary function, arterial blood gas parameters, and QCT features were explored using Spearman correlation analysis. A Cox regression was used to explore the association between QCT

features and prognosis with adjustments for age, sex, body mass index, smoking status, fibrosis status, pulmonary function, and treatment history. Sample size determination adhered to the 10 events per variable criterion to ensure statistical robustness. Given the exploratory nature of this investigation, statistical corrections for multiple comparisons were intentionally omitted.

Results

Baseline Clinical Characteristics and Prognosis

A total of 356 patients with ASS-ILD (87 males; median age: 56 years) and 155 patients with MDA5-ILD (57 males; median age: 50 years) were included in this study. Among the patients with ASS-ILD, 124 (34.8%) had RP-ILD, while 69 (44.5%) MDA5-ILD patients presented with RP-ILD. Detailed demographic and clinical data are summarized in Table 1. Among the patients with ASS-ILD or MDA5-ILD, those with RP-ILD were older and had worse pulmonary function (low VC%, FVC%, TLC%, DLco%, and OI).

By April 2024 [median follow-up duration: 4.45 years (interquartile range: 3.30 years) for ASS-ILD; 4.05 years (interquartile range: 4.01 years) for MDA5-ILD], complete prognostic outcomes were available for 231 of 356 patients

Table 1 Baseline Characteristics of Patients with ASS-ILD or MDA5-ILD

Characteristics	ASS-ILD		P	MDA5-ILD		P
	Non-RP-ILD	RP-ILD		Non-RP-ILD	RP-ILD	
n	232	124		86	69	
Age (years), median (IQR)	55.00 (48.00, 62.00)	57.00 (51.00, 66.00)	0.018	47.50 (39.25, 54.00)	53.00 (45.00, 59.00)	0.001
Male, n (%)	62 (26.7%)	25 (20.2%)	0.170	31 (36.0%)	26 (37.7%)	0.834
BMI (kg/m ²), median (IQR)	24.40 (22.30, 27.03)	24.50 (23.20, 26.00)	0.646	22.81 (20.57, 24.73)	22.96 (20.90, 24.99)	0.663
Never-smoker, n (%)	76 (32.8%)	40 (32.3%)	0.949	27 (31.4%)	15 (21.7%)	0.231
VC%	73.35 (60.18, 86.63)	67.85 (57.78, 79.25)	0.031	80.41 ± 15.63	73.95 ± 12.63	0.052
FVC%	73.95 (60.35, 87.85)	69.20 (57.30, 82.00)	0.046	82.02 ± 16.30	75.78 ± 13.48	0.072
FEV ₁ %	72.62 ± 18.98	68.05 ± 17.78	0.064	78.50 (68.50, 87.50)	73.00 (62.80, 80.70)	0.046
FEV ₁ /FVC	80.76 (76.67, 84.87)	82.78 (78.22, 86.86)	0.074	80.67 ± 5.82	81.40 ± 7.92	0.649
TLC%, median (IQR)	69.00 (58.20, 81.45)	65.00 (56.00, 73.55)	0.010	80.15 (75.98, 90.25)	73.00 (63.65, 83.25)	0.057
DL _{CO} %, median (IQR)	59.00 (47.20, 70.60)	49.85 (41.98, 62.68)	0.001	59.90 (51.88, 72.45)	55.15 (48.45, 60.4)	0.076
OI, median (IQR)	400.00 (361.90, 434.29)	380.95 (314.29, 438.10)	0.017	403.63 (353.69, 437.02)	360.56 (301.43, 416.31)	0.007
ANA, n (%)	117 (50.4%)	58 (46.8%)	0.511	11 (12.8%)	9 (13.0%)	0.963
RO-52, n (%)	123 (53.0%)	67 (54.0%)	0.855	23 (26.7%)	24 (34.8%)	0.279
JOI, n (%)	55 (23.7%)	26 (21.0%)	0.557	0 (0.0%)	2 (2.9%)	0.383
SSA, n (%)	207 (89.2%)	118 (95.2%)	0.058	2 (2.3%)	2 (2.9%)	1.000
EJ, n (%)	15 (6.5%)	10 (8.1%)	0.574	1 (1.2%)	1 (1.4%)	1.000
Mi-2, n (%)	2 (0.9%)	3 (2.4%)	0.473	4 (4.7%)	4 (5.8%)	1.000
PM-SCL, n (%)	3 (1.3%)	3 (2.4%)	0.723	5 (5.8%)	4 (5.8%)	1.000
PL7, n (%)	7 (3.0%)	4 (3.2%)	1.000	0 (0.0%)	0 (0.0%)	/
PL12, n (%)	6 (2.6%)	3 (2.4%)	1.000	1 (1.2%)	0 (0.0%)	1.000
SSB, n (%)	6 (2.6%)	2 (1.6%)	0.830	0 (0.0%)	0 (0.0%)	/
Prednisone, n (%)	216 (93.1%)	120 (96.8%)	0.152	83 (96.5%)	69 (100.0%)	0.571
Immunosuppression, n (%)	111 (47.8%)	58 (46.8%)	0.847	48 (55.8%)	47 (68.1%)	0.118
Antifibrosis, n (%)	14 (6.0%)	7 (5.6%)	0.882	1 (1.2%)	3 (4.3%)	0.463
Fibrosis, n (%)	102 (44.0%)	67 (54.0%)	0.070	20 (23.3%)	28 (40.6%)	0.020

Notes: Immunosuppression is defined as cyclophosphamide, ciclosporin, azathioprine, mycophenolate mofetil, tacrolimus, or hydroxychloroquine. Antifibrosis is defined as pirfenidone. Fibrosis is defined when the volume of reticular and honeycomb is more than 5% of whole lung. Continuous variables were succinctly depicted using means coupled with their respective standard deviations in cases of normal distribution, whereas medians along with interquartile range were employed for non-normally distributed data. Categorical variables were diligently presented as absolute numbers and corresponding percentages. Comparisons of data were meticulously executed, harnessing the power of statistical tests such as the Student's *t*-test or Mann-Whitney *U*-test for continuous variables, and the chi-square or Yates' correction for categorical variables.

Abbreviations: RP-ILD, rapid progressive interstitial lung disease; ASS-ILD, anti-synthetase syndrome related interstitial lung disease; MDA5-ILD, anti-melanoma differentiation-associated gene 5 antibody-positive dermatomyositis related interstitial lung disease; VC%, the proportion of actual value to the expected value for vital capacity; FVC%, the proportion of actual value to the expected value for forced vital capacity; FEV₁%, the proportion of actual value to the expected value for forced expiratory volume in the first second; FEV₁/FVC, the proportion of forced expiratory volume in the first second to the forced vital capacity; TLC%, the proportion of actual value to the expected value for total lung capacity; DL_{CO}%, the proportion of actual value to the expected value for carbon monoxide diffusing capacity; OI, oxygenation index; ANA, Anti-nuclear antibody; RO-52, Anti-RO-52 antibody; JOI, Anti-JO-1 antibody; SSA, Anti-Sjögren's-syndrome-related antigen A antibody; EJ, Anti-EJ antibody; Mi-2, Anti-Mi-2 antibody; PM-SCL, Anti-PM-SCL antibody; PL12, Anti-PL-12 antibody; IQR, interquartile ranges.

with ASS-ILD, of whom 31 were deceased and 12 had been admitted to the ICU once at least. Of the 31 patients who died, 13 developed RP-ILD. Of the 12 patients admitted to the ICU, 10 had RP-ILD. Of 155 patients with MDA5-ILD, we collected complete prognostic outcomes for 116 patients, of whom 21 died and 11 were admitted to the ICU. These 21 deaths included 12 patients with RP-ILD and 7 of 11 ICU events were RP-ILD cases. Compared with patients with ASS-ILD and MDA5-ILD without RP-ILD, those with RP-ILD were associated with higher mortality ([Supplementary Figure 2](#)).

Quantitative Imaging Markers in Prediction of RP-ILD

After conducting multiple corrections ([Table 2](#) and [Supplementary Table 1](#) and [2](#)), the volumes and percentage of GGO and consolidation on baseline HRCT in all patients with RP-ILD were significantly higher ($P < 0.001$) than those without RP-ILD. Furthermore, similar results and feature distributions were observed in patients with ASS-ILD and MDA5-ILD ([Supplementary Figures 3–7](#)).

As shown in [Table 3](#) and [Supplementary Table 3](#) and [4](#), after adjusting age, gender, smoke status, body mass index, fibrosis status, prednisone uses, immunosuppressive agent uses, and anti-fibrosis medication uses, respectively, the volume and percentage of consolidation and GGO were risks to RP-ILD in patients with ASS-ILD. Moreover, this trend was linear in patients with ASS-ILD (P for trend < 0.05). [Table 4](#) shows that it was not the volume or percentage of consolidation and GGO but the heterogeneity of consolidation, which was the risk associated with RP-ILD in patients with MDA5-ILD.

Subgroup analysis indicated that the association between the percentage of GGO and RP-ILD risk was stronger in younger patients, female, non-smoker, and overweight patients ([Figure 2A](#)). Notably, the increased percentage of GGO in JO1-positive and RO52-positive patients was a stronger risk factor for RP-ILD ([Figure 2A](#)). However, in patients with MDA5-ILD, the association between the percentage of GGO and RP-ILD remained comparable in nearly all subgroups ([Figure 2B](#)). Regarding consolidation, we found that younger patients, females, non-smoker, lower body weight, absence of fibrosis, and use of immunosuppressants were associated with a higher risk of RP-ILD with an increased consolidation percentage in ASS-ILD ([Figure 2C](#)). In patients with MDA5-ILD, the association between consolidation percentage and

Table 2 Differences in Features of Ground-Glass Opacities and Consolidation Between RP-ILD and Non-RP-ILD in Patients with ASS-ILD and MDA5-ILD

Quantitative Features	Non-RP-ILD	RP-ILD	P
ASS-ILD			
Ground-glass opacity: volume (mL)	140.33	198.97	<0.001
Ground-glass opacity: percentage (%)	5.27	7.87	<0.001
Ground-glass opacity: heterogeneity	0.68	0.68	0.057
Consolidation: volume (mL)	35.04	44.16	<0.001
Consolidation: percentage (%)	1.24	1.63	<0.001
Consolidation: heterogeneity	0.71	0.69	0.041
MDA5-ILD			
Ground-glass opacity: volume (mL)	47.95	85.16	<0.001
Ground-glass opacity: percentage (%)	1.72	3.31	<0.001
Ground-glass opacity: heterogeneity	0.67	0.67	0.129
Consolidation: volume (mL)	24.51	38.80	<0.001
Consolidation: percentage (%)	0.83	1.33	<0.001
Consolidation: heterogeneity	0.69	0.69	0.128

Notes: Because it was a crude comparison, we used the Mann–Whitney U -tests of two independent samples for comparison. Median value were also presented.

Abbreviations: RP-ILD, rapid progressive interstitial lung disease; ASS-ILD, anti-synthetase syndrome related interstitial lung disease; MDA5-ILD, anti-melanoma differentiation-associated gene 5 antibody-positive dermatomyositis related interstitial lung disease.

Table 3 Association of Quantitative Ground-Glass Opacities and Consolidation on Baseline HRCT with RP-ILD in Patients with ASS-ILD

Quantitative Features on HRCT	Model-1	Model-2	Model-3	P for Trend
	OR (95% CI)	OR (95% CI)	OR (95% CI)	
Per SD	124/356	124/356	124/356	
Ground-glass opacity: volume (mL)	1.41 (1.12, 1.79)	1.39 (1.08, 1.77)	1.39 (1.08, 1.78)	0.003
Ground-glass opacity: percentage (%)	1.39 (1.11, 1.76)	1.36 (1.07, 1.73)	1.36 (1.06, 1.74)	0.007
Ground-glass opacity: heterogeneity	1.20 (0.95, 1.51)	1.15 (0.90, 1.47)	1.14 (0.89, 1.46)	0.316
Consolidation: volume (mL)	1.56 (1.22, 2.00)	1.54 (1.19, 1.99)	1.55 (1.20, 2.00)	<0.001
Consolidation: percentage (%)	1.63 (1.28, 2.09)	1.62 (1.25, 2.11)	1.63 (1.25, 2.12)	<0.001
Consolidation: heterogeneity	0.83 (0.66, 1.04)	0.82 (0.65, 1.02)	0.82 (0.65, 1.03)	0.009

Notes: Model-1: adjusted for age, gender, smoke status, and body mass index. Model-2: additionally adjusted fibrosis status based on Model-1. Model-3: additionally adjusted prednisone uses, immunosuppressive agent uses, and anti-fibrosis medication uses based on Model-2. The effect sizes of all models were calculated using 1 SD change of each quantitative HRCT feature. P for trend was conducted by separating each HRCT feature value into 4 categories according to its quantiles based on Model-3.

Abbreviations: HRCT, high-resolution computed tomography; RP-ILD, rapid progressive interstitial lung disease; ASS-ILD, anti-synthetase syndrome related interstitial lung disease; OR, odd ratio; 95% CI, 95% confidence interval; SD, standard difference.

Table 4 Association of Quantitative Ground-Glass Opacities and Consolidation on Baseline HRCT with RP-ILD in Patients with MDA5-ILD

Quantitative Features on HRCT	Model-1	Model-2	Model-3	P for Trend
	OR (95% CI)	OR (95% CI)	OR (95% CI)	
Per SD	69/155	69/155	69/155	
Ground-glass opacity: volume (mL)	1.61 (0.98, 2.66)	1.47 (0.91, 2.39)	1.50 (0.91, 2.49)	0.131
Ground-glass opacity: percentage (%)	1.66 (0.98, 2.80)	1.50 (0.89, 2.52)	1.54 (0.90, 2.64)	0.117
Ground-glass opacity: heterogeneity	1.26 (0.87, 1.81)	1.10 (0.72, 1.68)	1.18 (0.76, 1.83)	0.670
Consolidation: volume (mL)	1.38 (0.89, 2.14)	1.20 (0.75, 1.93)	1.27 (0.77, 2.12)	0.024
Consolidation: percentage (%)	1.33 (0.90, 1.96)	1.17 (0.77, 1.79)	1.25 (0.79, 1.97)	0.105
Consolidation: heterogeneity	1.53 (1.04, 2.25)	1.54 (1.05, 2.27)	1.49 (1.01, 2.21)	0.248

Notes: Model-1: adjusted for age, gender, smoke status, and body mass index. Model-2: additionally adjusted fibrosis status based on Model-1. Model-3: additionally adjusted immunosuppressive agent uses based on Model-2. The effect sizes of all models were calculated using 1 SD change of each quantitative HRCT feature. P for trend was conducted by separating each HRCT feature value into 4 categories according to its quantiles based on Model-3.

Abbreviations: HRCT, high-resolution computed tomography; RP-ILD, rapid progressive interstitial lung disease; MDA5-ILD, anti-melanoma differentiation-associated gene 5 antibody-positive dermatomyositis related interstitial lung disease; OR, odd ratio; 95% CI, 95% confidence interval; SD, standard difference.

RP-ILD remained stable in nearly all subgroups (Figure 2D), and the association between other quantitative metrics and RP-ILD among subgroups was also stable (Supplementary Tables 5–16).

The Association Between Quantitative Imaging Markers and Adverse Events

For patients with ASS-ILD (Table 5 and Supplementary Figure 2), an increase in the volume and percentage of GGO was a risk factor for poor prognosis, regardless of whether they experienced RP-ILD. In patients with ASS-ILD, an 1-standard-difference increase in GGO percentage was associated with a 112% (95% confidence interval: 46%–216%) increase in adverse events after adjusting for age, sex, smoking status, body mass index, fibrosis status, prednisone use, immunosuppressive agent use, and anti-fibrosis medication use in patients with previous RP-ILD. While the hazard ratio of per-standard-difference GGO percentage was 2.41 (95% confidence interval: 1.56 to 3.71) on adverse event risk for ASS-ILD patients without a history of RP-ILD. However, an increase in the volume and percentage of consolidation may not predict the risk of adverse events in ASS-ILD patients without RP-ILD.

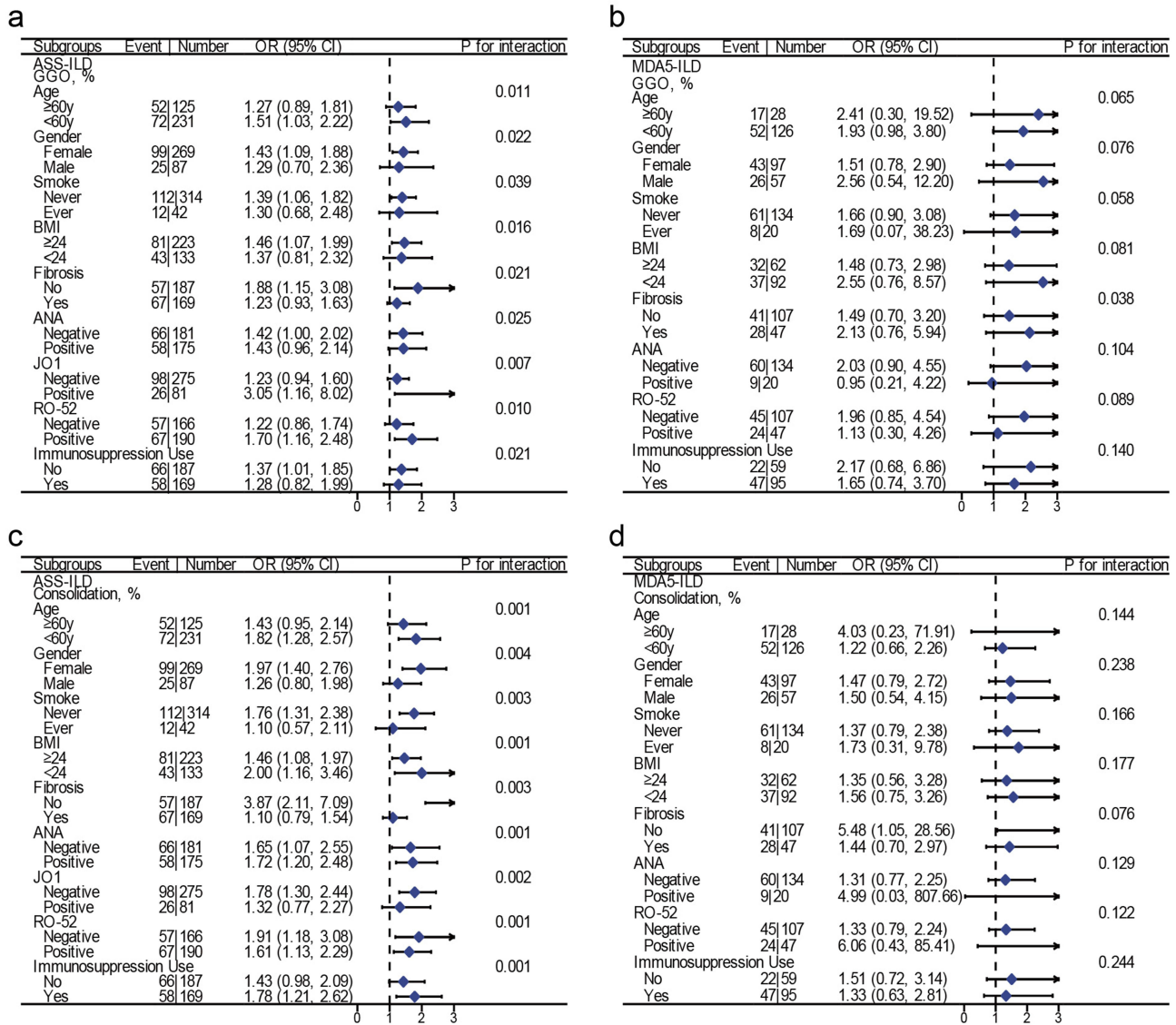


Figure 2 Association between quantitative features of GGO and consolidation and RP-ILD among patients with ASS-ILD or MDA5-ILD. We adjusted age, gender, smoke status, body mass index, fibrosis status, prednisone uses (ASS-ILD only), immunosuppressive agent uses, and anti-fibrosis medication uses (ASS-ILD only) to estimate the effect of GGO and consolidation percentage on the RP-ILD excluding the stratum factor. The effect sizes of all models were calculated using 1 SD change of each quantitative HRCT feature. (a) The percentage of GGO in ASS-ILD. (b) The percentage of GGO in MDA5-ILD. (c) The percentage of consolidation in ASS-ILD. (d) The percentage of consolidation in MDA5-ILD. Immunosuppression is defined as cyclophosphamide, ciclosporin, azathioprine, mycophenolate mofetil, tacrolimus, or hydroxychloroquine. **Abbreviations:** GGO, ground glass opacity; RP-ILD, rapid progressively interstitial lung disease; ASS-ILD, anti-synthetase syndrome related interstitial lung disease; MDA5-ILD, anti-melanoma differentiation-associated gene 5 antibody-positive dermatomyositis related interstitial lung disease; BMI, Body mass index; ANA, Anti-nuclear antibody; RO-52, Anti-RO-52 antibody; JO1, Anti-JO-1 antibody.

For MDA5-ILD patients with previous RP-ILD (Table 6 and Supplementary Figure 2), the volume, percentage, and mass of GGO were risk factors for adverse events. An one standard difference increase in GGO percentage was associated with a 1.32-fold increase in adverse events (95% confidence interval: 1.45-3.27). In contrast, for MDA5-ILD patients without previous RP-ILD, neither GGO nor consolidation was a risk factor for adverse events.

Discussion

In this study, we analyzed imaging markers, including GGO and consolidation on baseline HRCT, to predict RP-ILD and adverse events in patients with ASS-ILD and MDA5-ILD. Critically, elevated GGO/consolidation percentage demonstrated divergent prognostic relevance: in ASS-ILD, these metrics independently predicted poor outcomes regardless of

Table 5 Association Between the Baseline Ground-Glass Opacity, Consolidation and Adverse Events in Patients with ASS -ILD

Baseline Features on HRCT	Non-RP-ILD				RP-ILD			
	Model-1 HR (95% CI)	Model-2 HR (95% CI)	Model-3 HR (95% CI)	P for Trend	Model-1 HR (95% CI)	Model-2 HR (95% CI)	Model-3 HR (95% CI)	P for Trend
Ground-glass opacity: percentage (%)	2.23 (1.61, 3.10)	2.23 (1.51, 3.28)	2.41 (1.56, 3.71)	<0.001	2.11 (1.43, 3.10)	2.10 (1.45, 3.06)	2.12 (1.42, 3.16)	0.035
Ground-glass opacity: volume (mL)	2.50 (1.72, 3.63)	2.61 (1.68, 4.05)	2.56 (1.63, 4.04)	<0.001	1.86 (1.29, 2.69)	1.76 (1.25, 2.48)	1.75 (1.22, 2.51)	0.059
Ground-glass opacity: heterogeneity	1.06 (0.61, 1.85)	0.96 (0.54, 1.70)	0.73 (0.38, 1.41)	0.121	1.05 (0.66, 1.67)	0.99 (0.61, 1.62)	1.07 (0.63, 1.79)	0.931
Consolidation: percentage (%)	2.16 (1.22, 3.82)	1.88 (1.02, 3.48)	1.92 (0.97, 3.83)	0.016	0.90 (0.60, 1.37)	0.98 (0.63, 1.50)	1.00 (0.64, 1.56)	0.712
Consolidation: volume (mL)	1.92 (1.13, 3.28)	1.65 (0.93, 2.96)	1.50 (0.79, 2.81)	0.237	0.81 (0.52, 1.26)	0.91 (0.57, 1.44)	0.90 (0.56, 1.46)	0.744
Consolidation: heterogeneity	1.06 (0.65, 1.73)	1.01 (0.62, 1.66)	1.02 (0.60, 1.74)	0.463	0.39 (0.23, 0.68)	0.42 (0.24, 0.73)	0.40 (0.22, 0.72)	0.015

Notes: Model-1: adjusted for age, gender, smoke status, and body mass index. Model-2: additionally adjusted FVC%, DL_{CO}%, OI based on Model-1. Model-3: additionally adjusted prednisone uses, immunosuppressive agent uses, and anti-fibrosis medication uses based on Model-2. The effect sizes of all models were calculated using 1 standard difference change of each quantitative HRCT feature. P for trend was conducted by separating each HRCT feature value into 4 categories according to its quantiles.

Abbreviations: HRCT, high-resolution computed tomography; ASS-ILD, anti-synthetase syndrome-related interstitial lung disease; RP-ILD, Rapid progressive interstitial lung disease; HR, hazard ratio; 95% CI, 95% confidence interval; FVC%, the proportion of actual value to the expected value for forced vital capacity; DL_{CO}%, the proportion of actual value to the expected value for carbon monoxide diffusing capacity; OI, oxygenation index; SD, standard difference.

Table 6 Association Between Ground-Glass Opacity, Consolidation and Adverse Events in Patients with MDA5-ILD

The Baseline Features on HRCT	Non-RP-ILD				RP-ILD			
	Model-1 HR (95% CI)	Model-2 HR (95% CI)	Model-3 HR (95% CI)	P for Trend	Model-1 HR (95% CI)	Model-2 HR (95% CI)	Model-3 HR (95% CI)	P for Trend
Ground-glass opacity: percentage (%)	0.47 (0.10, 2.18)	0.38 (0.06, 2.47)	0.29 (0.03, 2.65)	0.782	1.93 (1.27, 2.93)	2.17 (1.40, 3.36)	2.32 (1.45, 3.70)	0.753
Ground-glass opacity: volume (mL)	0.48 (0.11, 2.15)	0.40 (0.06, 2.42)	0.30 (0.04, 2.61)	0.898	1.68 (1.08, 2.62)	1.97 (1.23, 3.15)	2.05 (1.26, 3.36)	0.483
Ground-glass opacity: heterogeneity	1.17 (0.59, 2.33)	0.97 (0.41, 2.27)	1.13 (0.44, 2.91)	0.958	0.93 (0.65, 1.34)	0.93 (0.64, 1.35)	0.91 (0.61, 1.36)	0.488
Consolidation: percentage (%)	2.00 (0.71, 5.66)	1.34 (0.31, 5.81)	1.56 (0.31, 7.86)	0.604	1.24 (0.85, 1.80)	1.44 (0.94, 2.21)	1.51 (0.97, 2.35)	0.929
Consolidation: volume (mL)	2.53 (0.75, 8.56)	1.90 (0.36, 10.12)	2.29 (0.40, 13.14)	0.331	1.08 (0.76, 1.54)	1.20 (0.81, 1.76)	1.23 (0.82, 1.84)	0.707
Consolidation: heterogeneity	1.11 (0.59, 2.11)	1.08 (0.56, 2.07)	1.03 (0.55, 1.96)	0.663	0.65 (0.38, 1.09)	0.60 (0.35, 1.03)	0.57 (0.32, 1.00)	0.103

Notes: Model-1: adjusted for age, gender, smoke status, and body mass index. Model-2: additionally adjusted FVC%, DL_{CO}%, OI based on Model-1. Model-3: additionally adjusted prednisone uses, immunosuppressive agent uses, and anti-fibrosis medication uses based on Model-2. The effect sizes of all models were calculated using I standard difference change of each quantitative HRCT feature. P for trend was conducted by separating each HRCT feature value into 4 categories according to its quantiles.

Abbreviations: HRCT, high-resolution computed tomography; RP-ILD, rapid progressive interstitial lung disease; MDA5-ILD, anti-melanoma differentiation-associated gene 5 antibody-positive dermatomyositis related interstitial lung disease; HR, hazard ratio; 95% CI, 95% confidence interval; FVC%, the proportion of actual value to the expected value for forced vital capacity; DL_{CO}%, the proportion of actual value to the expected value for carbon monoxide diffusing capacity; OI, oxygenation index; SD, standard difference.

RP-ILD history, whereas in MDA5-ILD, significant mortality associations emerged exclusively in patients with prior RP-ILD episodes. This findings validated our hypothesis and provided clues for further study.

The core finding reveals that baseline volumes and percentages of GGO and consolidation on baseline HRCT are significantly higher in patients with RP-ILD than in non-RP-ILD patients. This aligns with the consensus in polymyositis-associated ILD literature, confirming that radiological severity serves as a universal warning sign for RP-ILD.^{1,37–39} GGO is the most common feature of HRCT in Chinese patients with ASS-ILD.⁴⁰ GGO and consolidation in quantitative HRCT metrics can predict RP-ILD in patients with ASS-ILD and MDA5-ILD.⁴¹ However, similar results in our study were observed only in the patients with ASS without RP-ILD. For MDA5 patients, a small amount of GGO exists in nearly all patients without RP-ILD who can live a long life with no additional risk derived from GGO. This phenomenon challenges the conventional assumption that extensive alveolar damage invariably precedes RP-ILD. Mechanistically, this paradox may stem from MDA5+ RP-ILD's fulminant pathogenesis: characterized by explosive alveolar-capillary injury, its progression often outpaces detectable morphological accumulation on imaging. This process is driven by MDA5-triggered neutrophil extracellular trap and dendritic cells producing interferon- α ⁴² that induce lung injury, coagulopathy, and rapid pulmonary failure.⁴³

To our knowledge, this is the first long-term follow-up study (median > 4 years) with the largest cohort of patients with MDA5-ILD and ASS-ILD. The prognostic warning value of GGO demonstrates universality but context-dependency. In a study using QCT, Xu et al⁴⁴ found that in patients with MDA5+, GGO and consolidation were significantly correlated with 6-month mortality. Higher HRCT score is associated with mortality in patients with MDA5-ILD in Chinese populations from Shanghai^{45,46} and Tianjin.⁴⁷ Previous studies most derive computed tomography score via visual assessment without accurate quantitation of specific lesions. The inability of current visual CT evaluation paradigms to discern individuals likely to experience poor outcomes during the early disease phase represents a major limitation in clinical practice. Our study, demonstrating the discriminatory prognostic power of quantitative GGO analysis – particularly within specific serological contexts (ASS-ILD vs MDA5-ILD) – thus holds significant clinical promise for enabling timely, targeted therapeutic interventions.

In patients with ASS-ILD, elevated GGO burden consistently correlates with poor prognosis regardless of prior RP-ILD history, mechanistically reflecting persistent active alveolitis—T-lymphocyte/macrophage infiltration and progressive parenchymal damage driven by antisynthetase antibodies.⁴³ Conversely, in MDA5-ILD cohorts, the prognostic significance of GGO specifically manifests in survivors with prior RP-ILD. This observation resonates with the concept of “different pathological pattern to same radiological appearance”: such GGO no longer represents acute exudative inflammation but signifies irreversible architectural destruction or incipient fibrosis, marking residual organ dysfunction after immunosuppressive therapy—a pathological scar of aberrant tissue repair following inflammatory catastrophe.³⁹ Furthermore, the limited prognostic role of consolidation (which showed no significant association with survival in our analysis) may relate to its frequent correlation with transient organizing pneumonia, where potential resolvability reduces its utility for long-term risk stratification, thereby reinforcing GGO as a more reliable chronic injury indicator.³⁹ In summary, quantitative HRCT analysis demands divergent interpretive frameworks for ASS-ILD versus MDA5-ILD. For ASS-ILD: Baseline GGO/consolidation predicts both RP-ILD and long-term mortality, necessitating early intensified immunosuppression to interrupt inflammatory cascades. For MDA5-ILD: RP-ILD prediction requires integration of serological/kinetic markers (eg, ferritin surges), while GGO's prognostic value emerges only post-acute phase, suggesting survivors warrant surveillance for fibrosis progression and exploration of antifibrotic therapies.

Our study had some limitations. First, patients who were unable to complete lung function owing to severe disease were not included; therefore, our results cannot represent seriously ill patients. Therefore, we can use only 3 months as the RP-ILD criterion, which may not be suitable for all situations.⁴⁸ Second, we lost 25% of the patients during the follow-up period, mainly due to ASS-ILD, which may have caused a loss of follow-up bias. Third, this study was a single-center study, and the sample size of the internal validation cohort was limited; therefore, the model needs to be further validated by larger multicenter studies and external patient cohorts. Also, while our sample size met the 10 events per variable threshold to mitigate overfitting risks, larger multi-center cohorts remain desirable to enhance generalizability. Fourth, as an exploratory investigation targeting hypothesis generation, statistical corrections for multiple comparisons were purposefully omitted. These constraints, particularly regarding population representativeness and analytical conservatism, are inherent to preliminary biomarker research but do not invalidate the mechanistic insights presented. Fifth, our rigorous adjustment for key therapeutic variables including immunosuppressant types and dosing regimens, heterogeneity in adjunctive therapies—particularly ancillary interventions such as antifibrotic agent

initiation timing, pulmonary rehabilitation intensity, and rescue oxygen protocols—may constitute residual confounding. This variability stems partly from the observational nature of the study, wherein treatment decisions were tailored to individual clinical status rather than standardized protocols. Crucially, while such individualization reflects real-world practice patterns and enhances external validity, it inherently limits causal inference regarding therapeutic efficacy. Future prospective studies should implement protocol-driven therapeutic bundles to isolate specific treatment effects, though this must be balanced against ecological validity considerations in complex autoimmune conditions.

Conclusion

In conclusion, this study establishes the volume and percentage quantification of GGO and consolidation on baseline HRCT as novel, clinically significant prognostic markers for RP-ILD and adverse outcomes in patients with MDA5-ILD and ASS-ILD. Notably, our work represents the first comprehensive validation and direct comparison of both volumetric and proportional CT metrics specifically within these high-risk patient cohorts, providing a clearer hierarchy of predictive imaging features. The immediate clinical applicability lies in the ability of these readily quantifiable, non-invasive HRCT parameters to facilitate early risk stratification. This empowers clinicians to identify patients at imminent risk of devastating RP-ILD progression or mortality, thereby enabling prompt therapeutic intensification and tailored surveillance strategies. Thus, our findings bridge critical gaps in prognostication tools for these complex disorders, offering a practical radiological framework to guide aggressive management decisions at diagnosis.

Abbreviations

RP, rapid progression; ASS, anti-synthase syndrome; MDA5, anti-MDA5-positive dermatomyositis; GGO, ground glass opacity; IIM, idiopathic inflammatory myopathy; ILD, interstitial lung disease; HRCT, high-resolution computed tomography; QCT, quantitative CT; MDD, multi-disciplinary discussion; PaO₂, arterial oxygen tension; ICU, intensive care unit; PaCO₂, arterial carbon dioxide pressure; FiO₂, fraction of inhaled oxygen; ANA, anti-nuclear antibody; RO-52, anti-RO-52 antibody; JO-1, anti-JO-1 antibody; SSA, anti-Sjögren's-syndrome-related antigen A antibody; EJ, anti-EJ antibody; Mi-2, anti-Mi-2 antibody; PM-SCL, anti-PM-SCL antibody; PL-12, anti-PL-12 antibody; RP-ILD, rapid progressive interstitial lung disease; ASS-ILD, anti-synthetase syndrome related interstitial lung disease; OR, odd ratio; HR, hazard ratio; 95% CI, 95% confidence interval; FVC%, the proportion of actual value to the expected value for forced vital capacity; DL_{CO}%, the proportion of actual value to the expected value for carbon monoxide diffusing capacity; OI, oxygenation index; SD, standard difference; VC%, the proportion of actual value to the expected value for vital capacity; FEV1%, the proportion of actual value to the expected value for forced expiratory volume in the first second; FEV1/FVC, the proportion of forced expiratory volume in the first second to the forced vital capacity; TLC%, the proportion of actual value to the expected value for total lung capacity.

Data Sharing Statement

The authors intend to share individual deidentified participant data. The data includes clinical information, features from FACT AI+-digitalLung, or raw images. No other study documents will be made available. The data will be accessible from the corresponding author upon request (mikie0763@126.com and daihuaping@ccmu.edu.cn) with full protocols, ethics approvals, and conflicts of interest in your study. The data will be made available from the date this article published to June 30, 2027.

Ethics Approval and Informed Consent

The study protocol was approved by the hospital Ethics Committee (No. 2017-25) and was retrospectively analyzed based on the registered perspective cohort (NCT04370158). Written informed consent was obtained from all the patients.

Consent for Publication

Details of any images, videos, recordings, etc can be published.

Acknowledgments

We thank all the study participants, funding providers, and individuals who helped in performing this study.

Author Contributions

All authors made a significant contribution to the work reported, whether that is in the conception, study design, execution, acquisition of data, analysis and interpretation, or in all these areas; took part in drafting, revising or critically reviewing the article; gave final approval of the version to be published; have agreed on the journal to which the article has been submitted; and agree to be accountable for all aspects of the work.

Funding

This study was funded by National Key Technologies Research and Development Program Precision Medicine Research (2021YFC2500700 and 2016YFC0901101), National High Level Hospital Clinical Research Funding (2022-NHLHCRF-LX-01-0104), Noncommunicable Chronic Diseases-National Science and Technology Major Project (2024ZD0528901), BeiJing Natural Science Foundation (7244404), CAMS Institute of Respiratory Medicine Grant for Young Scholars (2023-ZF-16), and National Natural Science Foundation of China (82370072).

Disclosure

All authors declare no competing interests in this work.

References

1. Wu W, Guo L, Fu Y, et al. Interstitial lung disease in anti-MDA5 positive dermatomyositis. *Clin Rev Allergy Immunol*. 2021;60(2):293–304. doi:10.1007/s12016-020-08822-5
2. Douglas WW, Tazelaar H, Hartman T. Polymyositis-dermatomyositis-associated interstitial lung. *Am J Respir Crit Care Med*. 2001;164(7):1182–1185. doi:10.1164/ajrccm.164.7.2103110
3. Schmidt J. Current classification and management of inflammatory myopathies. *J Neuromuscul Dis*. 2018;5(2):109–129. doi:10.3233/JND-180308
4. Betteridge Z, McHugh N. Myositis-specific autoantibodies: an important tool to support diagnosis of myositis. *J Intern Med*. 2016;280(1):8–23. doi:10.1111/joim.12451
5. Lia Y, Fana Y, Wang Y, Yanga S, Dua X, Yea Q. Phenotypic clusters and survival analyses in interstitial pneumonia with myositis-specific autoantibodies. *Sarcoidosis Vasc Diffuse Lung Dis*. 2022;38(4):e2021047. doi:10.36141/svdl.v38i4.11368
6. Pinal-Fernandez I, Casal-Dominguez M, Mammen AL. Immune-mediated necrotizing myopathy. *Curr Rheumatol Rep*. 2018;20(4):21. doi:10.1007/s11926-018-0732-6
7. Baratella E, Marrocchio C, Cifaldi R, et al. Interstitial lung disease in patients with antisynthetase syndrome: a retrospective case series study. *Jpn J Radiol*. 2021;39(1):40–46. doi:10.1007/s11604-020-01030-3
8. Yoshida N, Okamoto M, Kaieda S, et al. Association of anti-aminoacyl-transfer RNA synthetase antibody and anti-melanoma differentiation-associated gene 5 antibody with the therapeutic response of polymyositis/dermatomyositis-associated interstitial lung disease. *Respir Investig*. 2017;55(1):24–32. doi:10.1016/j.resinv.2016.08.007
9. Marco JL, Collins BF. Clinical manifestations and treatment of antisynthetase syndrome. *Best Pract Res Clin Rheumatol*. 2020;34(4):101503. doi:10.1016/j.berh.2020.101503
10. Shi J, Li S, Yang H, et al. Clinical profiles and prognosis of patients with distinct antisynthetase autoantibodies. *J Rheumatol*. 2017;44(7):1051–1057. doi:10.3899/jrheum.161480
11. Hamaguchi Y, Fujimoto M, Matsushita T, et al. Common and distinct clinical features in adult patients with anti-aminoacyl-tRNA synthetase antibodies: heterogeneity within the syndrome. *PLoS One*. 2013;8(4):e60442. doi:10.1371/journal.pone.0060442
12. Kobayashi N, Takezaki S, Kobayashi I, et al. Clinical and laboratory features of fatal rapidly progressive interstitial lung disease associated with juvenile dermatomyositis. *Rheumatology*. 2015;54(5):784–791. doi:10.1093/rheumatology/keu385
13. Xu Y, Yang CS, Li YJ, et al. Predictive factors of rapidly progressive-interstitial lung disease in patients with clinically amyopathic dermatomyositis. *Clin Rheumatol*. 2016;35(1):113–116. doi:10.1007/s10067-015-3139-z
14. Lega JC, Reynaud Q, Belot A, Fabien N, Durieu I, Cottin V. Idiopathic inflammatory myopathies and the lung. *Eur Respir Rev*. 2015;24(136):216–238. doi:10.1183/16000617.00002015
15. Satoh T, Okano T, Matsui T, et al. Novel autoantibodies against 7SL RNA in patients with polymyositis/dermatomyositis. *J Rheumatol*. 2005;32(9):1727–1733.
16. Kalluri M, Sahn SA, Oddis CV, et al. Clinical profile of anti-PL-12 autoantibody. Cohort study and review of the literature. *Chest*. 2009;135(6):1550–1556. doi:10.1378/chest.08-2233
17. Won Huh J, Soon Kim D, Keun Lee C, et al. Two distinct clinical types of interstitial lung disease associated with polymyositis-dermatomyositis. *Respir Med*. 2007;101(8):1761–1769. doi:10.1016/j.rmed.2007.02.017
18. Koreeda Y, Higashimoto I, Yamamoto M, et al. Clinical and pathological findings of interstitial lung disease patients with anti-aminoacyl-tRNA synthetase autoantibodies. *Intern Med*. 2010;49(5):361–369. doi:10.2169/internalmedicine.49.2889
19. Ruaro B, Baratella E, Confalonieri P, et al. High-resolution computed tomography: lights and shadows in improving care for SSc-ILD patients. *Diagnostics*. 2021;11(11):1960. doi:10.3390/diagnostics11111960

20. Jacob J, Bartholmai BJ, Rajagopalan S, et al. Mortality prediction in idiopathic pulmonary fibrosis: evaluation of computer-based CT analysis with conventional severity measures. *Eur Respir J*. 2017;49(1):1601011. doi:10.1183/13993003.01011-2016
21. Clukers J, Lanclus M, Mignot B, et al. Quantitative CT analysis using functional imaging is superior in describing disease progression in idiopathic pulmonary fibrosis compared to forced vital capacity. *Respir Res*. 2018;19(1):213. doi:10.1186/s12931-018-0918-5
22. Yeo J, Yoon SH, Kim JY, et al. Quantitative interstitial lung disease scores in idiopathic inflammatory myopathies: longitudinal changes and clinical implications. *Rheumatology*. 2023;62(11):3690–3699. doi:10.1093/rheumatology/kead122
23. Handa T, Tanizawa K, Oguma T, et al. Novel artificial intelligence-based technology for chest computed tomography analysis of idiopathic pulmonary fibrosis. *Ann Am Thorac Soc*. 2022;19(3):399–406. doi:10.1513/AnnalsATS.202101-044OC
24. Bohan A, Peter JB. Polymyositis and dermatomyositis (first of two parts). *N Engl J Med*. 1975;292(7):344–347. doi:10.1056/nejm197502132920706
25. Mammen AL, Allenbach Y, Stenzel W, Benveniste O; Group EtWS. 239th ENMC international workshop: classification of dermatomyositis, Amsterdam, the Netherlands, 14–16 December 2018. *Neuromuscul Disord*. 2020;30(1):70–92. doi:10.1016/j.nmd.2019.10.005
26. Travis WD, Costabel U, Hansell DM, et al. An official American thoracic society/European respiratory society statement: update of the international multidisciplinary classification of the idiopathic interstitial pneumonias. *Am J Respir Crit Care Med*. 2013;188(6):733–748. doi:10.1164/rccm.201308-1483ST
27. Raghu G, Remy-Jardin M, Richeldi L, et al. Idiopathic pulmonary fibrosis (an Update) and progressive pulmonary fibrosis in adults: an official ATS/ERS/JRS/ALAT clinical practice guideline. *Am J Respir Crit Care Med*. 2022;205(9):e18–e47. doi:10.1164/rccm.202202-0399ST
28. Zuo Y, Ye L, Chen F, et al. Different multivariable risk factors for rapid progressive interstitial lung disease in anti-MDA5 positive dermatomyositis and anti-synthetase syndrome. *Front Immunol*. 2022;13:845988. doi:10.3389/fimmu.2022.845988
29. Moghadam-Kia S, Oddis CV, Sato S, Kuwana M, Aggarwal R. Antimelanoma differentiation-associated gene 5 antibody: expanding the clinical spectrum in north American patients with dermatomyositis. *J Rheumatol*. 2017;44(3):319–325. doi:10.3899/jrheum.160682
30. Huang K, Vinik O, Shojania K, et al. Clinical spectrum and therapeutics in Canadian patients with anti-melanoma differentiation-associated gene 5 (MDA5)-positive dermatomyositis: a case-based review. *Rheumatol Int*. 2019;39(11):1971–1981. doi:10.1007/s00296-019-04398-2
31. Yamaguchi K, Yamaguchi A, Kashiwagi C, et al. Differential clinical features of patients with clinically amyopathic dermatomyositis who have circulating anti-MDA5 autoantibodies with or without myositis-associated autoantibodies. *Respir Med*. 2018;140:1–5. doi:10.1016/j.rmed.2018.05.010
32. Motegi SI, Sekiguchi A, Toki S, et al. Clinical features and poor prognostic factors of anti-melanoma differentiation-associated gene 5 antibody-positive dermatomyositis with rapid progressive interstitial lung disease. *Eur J Dermatol*. 2019;29(5):511–517. doi:10.1684/ejd.2019.3634
33. Jiang L, Wang Y, Peng Q, Shu X, Wang G, Wu X. Serum YKL-40 level is associated with severity of interstitial lung disease and poor prognosis in dermatomyositis with anti-MDA5 antibody. *Clin Rheumatol*. 2019;38(6):1655–1663. doi:10.1007/s10067-019-04457-w
34. Moghadam-Kia S, Oddis CV, Sato S, Kuwana M, Aggarwal R. Anti-melanoma differentiation-associated gene 5 is associated with rapidly progressive lung disease and poor survival in US patients with amyopathic and myopathic dermatomyositis. *Arthritis Care Res*. 2016;68(5):689–694. doi:10.1002/acr.22728
35. Yu H, Yang Z, Wei Y, et al. Computed tomography-based radiomics improves non-invasive diagnosis of *Pneumocystis jirovecii* pneumonia in non-HIV patients: a retrospective study. *BMC Pulm Med*. 2024;24(1):11. doi:10.1186/s12890-023-02827-4
36. Yu F, Peng M, Bai J, et al. Comprehensive characterization of genomic and radiologic features reveals distinct driver patterns of RTK/RAS pathway in ground-glass opacity pulmonary nodules. *Int J Cancer*. 2022;151(11):2020–2030. doi:10.1002/ijc.34238
37. Tanizawa K, Handa T, Nakashima R, et al. HRCT features of interstitial lung disease in dermatomyositis with anti-CADM-140 antibody. *Respir Med*. 2011;105(9):1380–1387. doi:10.1016/j.rmed.2011.05.006
38. Tillie-Leblond I, Wislez M, Valeyre D, et al. Interstitial lung disease and anti-Jo-1 antibodies: difference between acute and gradual onset. *Thorax*. 2008;63(1):53–59. doi:10.1136/thx.2006.069237
39. Chen X, Jiang W, Jin Q, et al. Clinical, radiological and pathological features of anti-MDA5 antibody-associated interstitial lung disease. *RMD Open*. 2023;9(2):e003150. doi:10.1136/rmdopen-2023-003150
40. Wang R, Zhao Y, Qi F, et al. Analysis of the clinical features of antisynthetase syndrome: a retrospective cohort study in China. *Clin Rheumatol*. 2023;42(3):703–709. doi:10.1007/s10067-022-06404-8
41. Qiang Y, Wang H, Ni Y, et al. Development of a machine learning model in prediction of the rapid progression of interstitial lung disease in patients with idiopathic inflammatory myopathy. *Quant Imaging Med Surg*. 2024;14(12):9258–9275. doi:10.21037/qims-24-595
42. Lu X, Peng Q, Wang G. Anti-MDA5 antibody-positive dermatomyositis: pathogenesis and clinical progress. *Nat Rev Rheumatol*. 2024;20(1):48–62. doi:10.1038/s41584-023-01054-9
43. Wang G, McHugh NJ. An update on myositis autoantibodies and insights into pathogenesis. *Clin Exp Rheumatol*. 2025;43(2):364–371. doi:10.55563/clinexprheumatol/kjy2cy
44. Xu W, Wu W, Zhang D, et al. A novel CT scoring method predicts the prognosis of interstitial lung disease associated with anti-MDA5 positive dermatomyositis. *Sci Rep*. 2021;11(1):17070. doi:10.1038/s41598-021-96292-w
45. Zhou M, Ye Y, Yan N, Lian X, Bao C, Guo Q. Noninvasive positive pressure ventilator deteriorates the outcome of pneumomediastinum in anti-MDA5 antibody-positive clinically amyopathic dermatomyositis. *Clin Rheumatol*. 2020;39(6):1919–1927. doi:10.1007/s10067-019-04918-2
46. Zou J, Guo Q, Chi J, Wu H, Bao C. HRCT score and serum ferritin level are factors associated to the 1-year mortality of acute interstitial lung disease in clinically amyopathic dermatomyositis patients. *Clin Rheumatol*. 2015;34(4):707–714. doi:10.1007/s10067-015-2866-5
47. Tseng CW, Wang KL, Fu PK, et al. GAP score and CA-153 associated with one-year mortality in anti-MDA-5 antibody-positive patients: a real-world experience. *J Clin Med*. 2021;10(22):5241. doi:10.3390/jcm10225241
48. Jablonski R, Bhorade S, Streck ME, Dematte J. Recognition and management of myositis-associated rapidly progressive interstitial lung disease. *Chest*. 2020;158(1):252–263. doi:10.1016/j.chest.2020.01.033

International Journal of General Medicine

Publish your work in this journal

The International Journal of General Medicine is an international, peer-reviewed open-access journal that focuses on general and internal medicine, pathogenesis, epidemiology, diagnosis, monitoring and treatment protocols. The journal is characterized by the rapid reporting of reviews, original research and clinical studies across all disease areas. The manuscript management system is completely online and includes a very quick and fair peer-review system, which is all easy to use. Visit <http://www.dovepress.com/testimonials.php> to read real quotes from published authors.

Submit your manuscript here: <https://www.dovepress.com/international-journal-of-general-medicine-journal>

Dovepress
Taylor & Francis Group